

RESEARCH ARTICLE

Generation of an in vitro model of the outer annulus fibrosus-cartilage interface

Jasmine E. Chong^{1,2} | J. Paul Santerre^{2,3} | Rita A. Kandel^{1,2,4} 

¹Lunenfeld-Tanenbaum Research Institute, Mount Sinai Hospital, Toronto, Ontario, Canada

²Institute of Biomaterials and Biomedical Engineering, University of Toronto, Toronto, Ontario, Canada

³Translational Biology and Engineering Program and Faculty of Dentistry, University of Toronto, Toronto, Ontario, Canada

⁴Department of Laboratory Medicine and Pathobiology, University of Toronto, Toronto, Ontario, Canada

Correspondence

Rita A. Kandel Mount Sinai Hospital
600 University Ave, Ste 6-500 Toronto, ON
M5G 1X5, Canada.
Email: rita.kandel@sinaihealth.ca

Funding information

Canadian Institutes of Health Research, Grant/Award Number: MOP142325

Abstract

Current treatments for degenerative disc disease do not restore full biological functionality of the intervertebral disc (IVD). As a result, regenerative medicine approaches are being developed to generate a biological replacement that when implanted will restore form and function of the degenerated IVD. Tissue-engineered models to date have focused on the generation of nucleus pulposus and annulus fibrosus IVD components. However, these tissues need to be integrated with a cartilage endplate in order for successful implantation to occur. The purpose of this study was to generate an in vitro annulus fibrosus-cartilage interface model which would enable us to better understand the biological and biomechanical implications of such interfaces. It was hypothesized that in vitro-formed outer annulus fibrosus (OAF) and cartilage tissues would integrate in direct-contact coculture to yield an interface containing extracellular matrix with aspects resembling the native OAF-CEP interface. In vitro-formed tissues were generated using bovine OAF cell-seeded angle-ply, multi-lamellated polycarbonate urethane scaffolds and articular chondrocytes, which were then placed in direct-contact coculture. 2-week old OAF tissues integrated with 3-day old cartilage by 1 week of coculture. Immunohistochemical staining of 2-week interfaces showed that distributions of collagen type I, collagen type II, and aggrecan were similar to the native bovine interface. The apparent tensile strength of the in vitro interface increased significantly between 2 and 4 weeks of coculture. In summary, an annulus fibrosus-cartilage interface model can be formed in vitro which will facilitate the identification of conditions required to generate an entire tissue-engineered disc replacement suitable for clinical use.

KEYWORDS

biomaterials, bioreactors, extracellular matrix, tissue engineering

1 | INTRODUCTION

Intervertebral disc (IVD) and vertebral cartilage endplate degeneration are associated with chronic back pain, and are irreversible due to the inherent lack of regenerative capacity in these tissues.^{1,2} Conservative

treatments for chronic back pain do not target underlying degenerative processes, and surgical interventions do not guarantee pain relief and may lead to complications.^{3,4} As a result, there are a number of biologic approaches that are being investigated to repair/regenerate the damaged tissue including biomolecule injection, chondrocyte or

This is an open access article under the terms of the Creative Commons Attribution-NonCommercial License, which permits use, distribution and reproduction in any medium, provided the original work is properly cited and is not used for commercial purposes.

© 2020 The Authors. JOR Spine published by Wiley Periodicals, LLC on behalf of Orthopaedic Research Society JOR

stem cell injection, and gene therapy.⁵ Another possible approach is tissue engineering, a strategy aiming to generate a disc replacement that will restore IVD form and function and minimize further degeneration in adjacent discs.⁶

The IVD consists of the nucleus pulposus (NP) and surrounding annulus fibrosus (AF), with hyaline cartilage endplates (CEP) located on the cranial and caudal aspects (Figure 1). In contrast to the relatively homogenous NP, the AF is a multi-lamellar angle-ply structure organized into distinct inner and outer regions. Collagen fibers within successive AF lamellae are alternately oriented at $\pm 30^\circ$ angles with respect to the vertical axis.⁷ The outer AF (OAF) is predominately composed of highly aligned collagen type I fibers and contains elongated fibroblast-like cells. The inner AF (IAF) is less organized and contains collagen type I, collagen type II, proteoglycans, and rounded cells.^{8,9} The main proteoglycan of the IVD and CEP is aggrecan, which provides compressive resistance.¹⁰ The CEP is the site of attachment and mechanical load transfer between the soft IVD and stiff vertebral bone (VB).¹¹⁻¹⁴ AF fibers insert into the CEP and into the bone for further anchorage of the disc.^{13,15} Tissue engineering this interface remains a key challenge in developing a functional biological IVD replacement.

Tissue-engineered cell-based IVD models to date have focused on trying to reproduce some components of the disc.¹⁶⁻²¹ Concentric multi-lamellar angle-ply scaffolds have mimicked the AF's structural complexity using electrospun nanofibrous polymer scaffolds.²²⁻²⁸ NP components have been made from acellular or cell-seeded hydrogels or biomaterial scaffolds,^{20,26-31} and scaffold-free bioengineered NP-like tissues have been used to generate AF-NP constructs.²¹ However, there have been few attempts to include a CEP-like component. Hamilton et al created a NP-cartilage model in vitro that suggests it is possible to create this interface.³² More recently, an acellular porous polymer endplate was incorporated into a disc-like angle-ply structure, which was shown to improve implant integration into adjacent vertebrae in vivo.²⁸ The CEP should be included in a tissue-engineered disc replacement in order to establish proper biomechanics during loading and to facilitate nutrient diffusion. An in vitro study using the NP-cartilage-bone substitute model system showed that chondrocytes

produce a factor that inhibits proinflammatory $\text{TNF}\alpha$ production by NP cells and enhances NP proteoglycan content, suggesting that absence of a CEP may promote degeneration of an implant.³³ Furthermore, implanted in vitro-generated AF-NP tissues did not integrate continuously with the native rat endplate in vivo until 6 months post-operatively.¹⁸ Generation of the IVD-CEP interface in vitro may circumvent this slow process of postimplantation integration.

To the best of our knowledge, no study has described an integrated cell-based AF-CEP interface model. Our lab previously developed the methods to form in vitro multi-lamellated AF tissue^{21,22} and in vitro hyaline cartilage from primary chondrocytes in three-dimensional (3D) culture.³² Thus, the study hypothesis was that direct-contact coculture of in vitro-formed OAF tissue generated using aligned nanofibrous multi-lamellated angle-ply polycarbonate urethane (PU) scaffolds with in vitro-formed cartilage tissue will generate an integrated interface containing extracellular matrix (ECM) that resembles aspects of native OAF-CEP, and whose mechanical strength will improve over culture time.

2 | METHODS

2.1 | Generation of angle-ply nanofibrous PU scaffold constructs

Anionic dihydroxyl oligomer (ADO) and PU were synthesized as described previously.^{21,34} PU-ADO (0.15% ADO by dry weight of PU) was dissolved in 1,1,1,3,3,3-hexafluoro-2-propanol (105 228, Sigma-Aldrich, St. Louis, Missouri) to yield 18% concentration by dry weight of PU-ADO. Aligned nanofibrous scaffolds were produced by electrospinning the polymer solution for 8 hours onto a 1150 rpm rotating mandrel (17 kV applied potential difference, 0.5 mL/hr infusion rate). Scaffolds were posttreated in an Isotemp Vacuum Oven (Model 281A, Fisher Scientific, Pittsburgh, Pennsylvania) overnight at 45°C . 3×50 mm scaffold strips were cut at a 30° angle relative to nanofiber direction, and sterilized by gamma irradiation (2.5 Mrad). Irradiated scaffold strips were soaked in

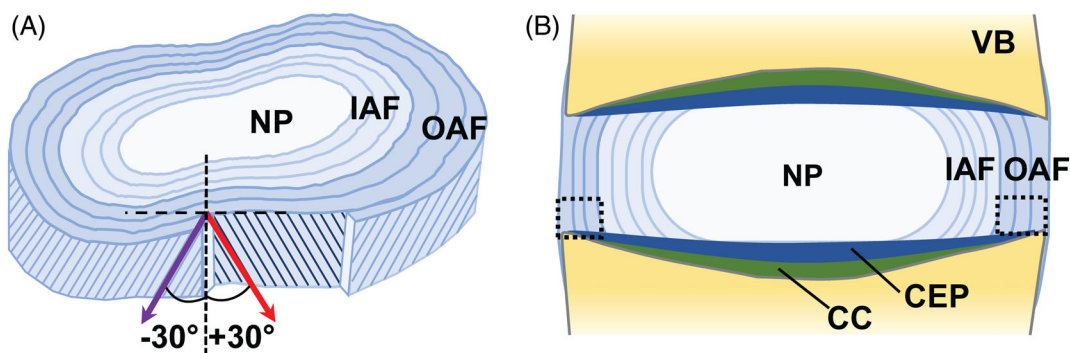


FIGURE 1 Schematic diagrams of the native IVD. A, The IVD consists of the nucleus pulposus (NP), and the multilamellar annulus fibrosus which is divided into inner (IAF) and outer (OAF) regions. Collagen fibers between successive lamellae are oriented at opposing 30° angles. B, The IVD is attached to the vertebral bone (VB) through hyaline cartilage endplates (CEP). A layer of calcified cartilage (CC) lies between the hyaline CEP and VB. The dotted black boxes indicate the OAF-CEP interface region

10 $\mu\text{g}/\text{mL}$ fibronectin (f1141, Sigma-Aldrich) in sterile phosphate buffered saline without Ca^{2+} or Mg^{2+} (PBS-/-; Wisent, St-Bruno, Quebec) overnight at 37°C. Two fibronectin-coated strips were stacked with opposing fiber angle orientation and rolled loosely around TYGON 3350 tubing (4 mm outer diameter; Saint-Gobain, Beaverton, Michigan) to create individual six-layered concentric constructs (Figure 2).

2.2 | Formation of multi-lamellated OAF-like tissues

IVDs were aseptically excised from 6 to 9-month old bovine caudal spines and placed in Ham's F12 media (Wisent). OAF tissues (distinguished from IAF during dissection by their distinct texture) were finely diced and digested at 37°C in 0.3% protease (P5147; Sigma) for 1 hour at 37°C, followed by 0.2% collagenase A (COLLA-RO; Roche, Mannheim, Germany) overnight at 37°C. Cells were filtered through a sterile mesh, washed three times, and resuspended at 1.6×10^6 cells/mL in Dulbecco's modification Eagle's medium (DMEM [4.5 g/L glucose]; Wisent) supplemented with 5% fetal bovine serum (FBS; Wisent). Eight scaffold constructs were secured by pins within a spinning bioreactor. 8×10^6 OAF cells in suspension were added and scaffolds were dynamically seeded in each bioreactor containing 45 mL of AF-optimized complete media (DMEM, supplemented with 10% FBS, 1% ITS [315-080-ZL, Wisent], 1% sodium pyruvate [11360-070, Gibco, Grand Island, New York], 0.1 μM dexamethasone [D2915, Sigma], 40 $\mu\text{g}/\text{mL}$ L-proline [P5607, Sigma], and 1% Antibiotic-Antimycotic solution [450-115-EL, Wisent]). After 2 days, the full volume was replaced with fresh complete media containing 100 $\mu\text{g}/\text{mL}$ ascorbic acid (Sigma-Aldrich). Two-thirds of the volume was replaced every 2 to 3 days. Tissues were maintained in dynamic culture at 35 rpm for 2 weeks (Figure 2).

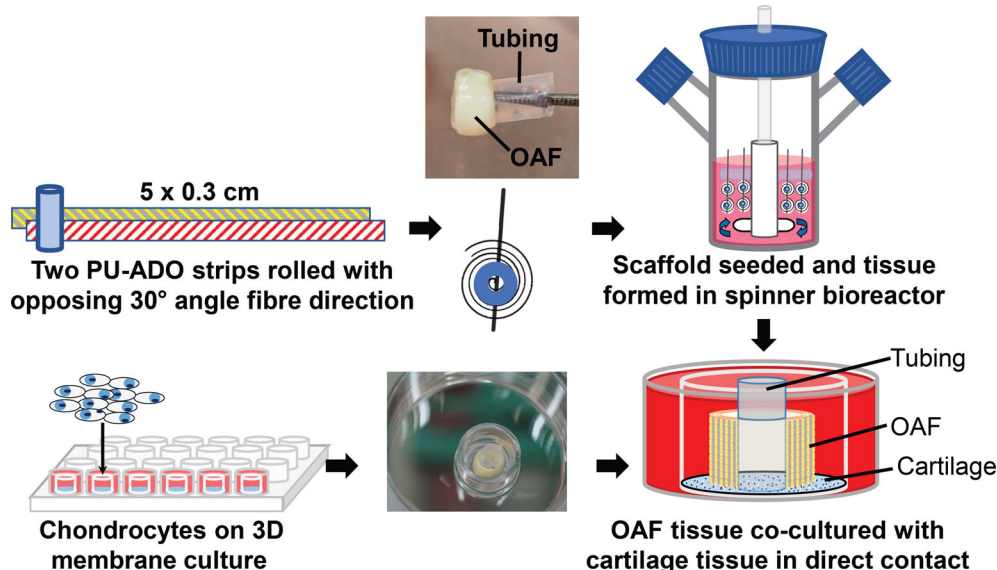
2.3 | Formation of hyaline-like cartilage tissue in 3D culture

Full-thickness cartilage harvested from 6 to 9-month old bovine metacarpal-phalangeal joints was placed in Ham's F12. Tissues were digested at 37°C in 0.25% protease for 1 hour followed by 0.1% collagenase A overnight. Cells were filtered, washed three times in Ham's F12, and placed in cryomedia (50% DMEM, 40% FBS, 10% DMSO) at 5×10^6 cells per cryotube at -80°C until use. Frozen chondrocytes were thawed, pelleted, washed immediately, and allowed to recover in Ham's F12 media for at least 10 minutes. 1×10^6 cells were seeded on type II collagen-coated Millicell membrane inserts (0.4 μm pore size, 12 mm diameter; Millipore, Cork, Ireland) in Ham's F12, 10% FBS. After 2 days, the media was replaced with fresh Ham's F12, 10% FBS, and ascorbic acid (final concentration 100 $\mu\text{g}/\text{mL}$). Media was replaced every 2 to 3 days.

2.4 | Fluorescent labelling of primary chondrocytes

Select cultures of freshly isolated chondrocytes (1×10^6 cells/mL) were incubated at 37°C for 10 minutes in 2.5 μM carboxyfluorescein diacetate (CFDA; V12883, Invitrogen, Eugene, Oregon) in PBS-/-, protected from light as described previously.³⁵ Chondrocytes were centrifuged at 600 RCF and washed twice for 30 minutes in Ham's F12 at 37°C. Visualization and counting of the cells using differential interference contrast (DIC) and fluorescent microscopy (Model IX81, Olympus, Waltham, Massachusetts) with OptiGrid imaging confirmed that >95% of aliquoted chondrocytes were labeled (data not shown). Labeled chondrocytes were resuspended in Ham's F12 supplemented with 10% FBS and seeded on membrane inserts as described above.

FIGURE 2 Schematic of culture method. Two strips of PU-ADO aligned nanofibrous scaffolds were stacked and rolled together around a 6 mm-long TYGON tube to form six-layered angle-ply constructs. Primary bovine OAF cells were seeded and cultured within a spinning bioreactor for 2 weeks. Articular chondrocytes were cultured on membrane inserts for 3, 5, or 7 days. 2-week old OAF tissue was placed on the cartilage tissue within each membrane insert holder in a six-well plate. The tissues were cocultured in direct contact for various times up to 4 weeks



2.5 | Static coculture of in vitro-formed OAF and cartilage tissues

In a six-well plate, 2-week old OAF tissue constructs formed around TYGON tubing were placed in direct contact with 3, 5, or 7-day old cartilage on each membrane (Figure 2). Five milliliters of DMEM complete media with 100 µg/mL ascorbic acid was pipetted in the well, around the outside of the membrane. One hundred and eighty microliters was placed on the membrane, submerging the OAF. After 48 hours, the final volume was brought up to 10 mL. Half the volume was replaced with fresh complete media every 2 to 3 days. Cocultured tissues and control OAF and cartilage tissues were grown separately under static culture conditions and were harvested at various times up to 4 weeks.

2.6 | Pull-apart testing of OAF-CEP constructs

Axial tensile strength testing was conducted using an Instron mechanical tester (Model 4301, Instron, Norwood, Massachusetts) at room temperature. Samples were kept hydrated in media until immediately before testing. Excess media was blotted away, and the top and bottom of each construct was fixed to the machine jig using Crazy Glue® gel. The glue was allowed to cure for 5 minutes under a preload of ~0.1 N. Tensile strain was applied at 1 mm/minute with a 50 N capacity load cell (full scale = 2.5 N) until OAF and cartilage tissues were completely separated. Testing for each sample was completed within approximately 10 minutes, and tissues remained moist. Normalized kPa stress values were calculated from maximum force values of force-displacement graphs and the contact surface area (SA) of each detached OAF. Afterward, the contact area of each OAF was painted with black ink and photographed with an Olympus OM-D E-M10 II camera. Each sample image was traced three times using ImageJ software to obtain an average SA value. Samples that did not fully separate during tensile testing were processed for histological examination to determine the site of early failure and were not included in the calculation of tensile strength.

2.7 | Histological characterization of native and in vitro OAF-CEP interface

In vitro-formed tissues were fixed in 10% buffered formalin for 1 hour and immersed in 30% sucrose overnight at 4°C. Native bovine (6-9 months old) caudal IVD-CEP-VB segments were fixed in 10% buffered formalin for 48 hours, decalcified in 0.5 M EDTA for 4 weeks, and immersed in 30% sucrose for 48 hours. Tissues were embedded in Optimal Cutting Temperature Compound embedding medium and maintained at -30°C. Seven micrometer thick sagittal frozen sections were mounted on cryotape³⁶ (Cryofilm type 2C, SECTION-LAB Co. Ltd., Hiroshima, Japan) and adhered onto glass slides using UV-activated optical glue (Norland Optical Adhesive 61, Norland Products Inc., Cranbury, New Jersey) as previously described.³⁷ Adhered sections were rehydrated with double-distilled water and stained with hematoxylin and eosin (H&E) or toluidine blue, and imaged by light microscopy.

2.8 | Immunohistochemical characterization of the OAF-CEP interface model

Antigen retrieval was used for immunostaining for collagen types I and II as follows: pepsin (2.5 mg/mL in TBS pH 2.0; P7012, Sigma) for 10 minutes at room temperature; two 10-minute washes in PBS-/-; trypsin (2.5 mg/mL in TBS; T7409, Sigma) for 30 minutes at room temperature; one 5-minute wash; and hyaluronidase (25 mg/mL in PBS -/-; H3506, Sigma) for 30 minutes at 37°C; one 5-minute wash. For aggrecan immunostaining, sections underwent the hyaluronidase predigestion only. Sections were blocked with 20% goat serum and 0.1% Triton X-100 in PBS-/- for 1 hour at room temperature, washed for 5 minutes and incubated overnight at 4°C with antibodies reactive with collagen type I (1:75 dilution; ab34710, Abcam, Cambridge, Massachusetts), collagen type II (1:75 dilution; MAB8887, Millipore, Temecula, California), or aggrecan (1:750 dilution; AHP002, Life Technologies, Frederick, Maryland) in diluent (10% goat serum, 0.1% Triton X-100 in PBS-/-). Rabbit or mouse IgG was used as the primary antibody negative control depending on the source of primary antibody. Sections were washed three times and incubated for 1 hour at room temperature with fluorophore-labeled secondary antibodies (1:1000 dilution; goat anti-mouse IgG A11032 or goat anti-rabbit IgG A11008, Life Technologies, Eugene, Oregon), followed by nuclear staining with DAPI (1:10000 in PBS-/-) for 5 minutes. Immunostained sections were visualized under a Zeiss Axioplan fluorescent microscope.

2.9 | Quantification of DNA, collagen, and proteoglycan contents

In vitro OAF-CEP tissues were excised from the membranes. To isolate the tissue interface region, 1 mm of OAF tissue above the cartilage layer was cut under a dissecting microscope. Three and seven millimeter diameter biopsy punches were used to remove the cartilage inside (in the lumen of the circularized OAF) and outside and around the OAF tissue, respectively (Figure S1). Control in vitro cartilage and OAF tissues cultured alone under identical culture conditions for the same time period were cut similarly to generate tissues of similar dimensions. Tissues were digested in 40 µg/mL papain (P3125, Sigma) in digestion buffer (35 mM ammonium acetate, 1 mM EDTA, 2 mM DTT pH 6.2) for 48 hours at 65°C. DNA content was determined by a fluorometric assay (355 nm excitation, 460 nm emission) using Hoechst 33258 dye as previously described.²¹ Sulphated glycosaminoglycan (GAG) content was determined using a dimethylmethylene blue binding assay and spectrophotometry ($\lambda = 525$ nm).²¹ To determine hydroxyproline (OH-Pro) content, papain-digested samples were hydrolyzed in an equal volume of 6 N hydrochloric acid at 110°C for 18 hours, followed by neutralization with the same volume of 5.7 N sodium hydroxide. OH-Pro content was quantified using the chloramine-T/Ehrlich's reagent assay and spectrophotometry ($\lambda = 560$ nm).²¹ Calf thymus DNA (D1501, Sigma), bovine trachea chondroitin sulphate A (C8529, Sigma), and *Cis*-4-hydroxy-L-proline (219959, Aldrich) were used to generate standard curves for DNA,

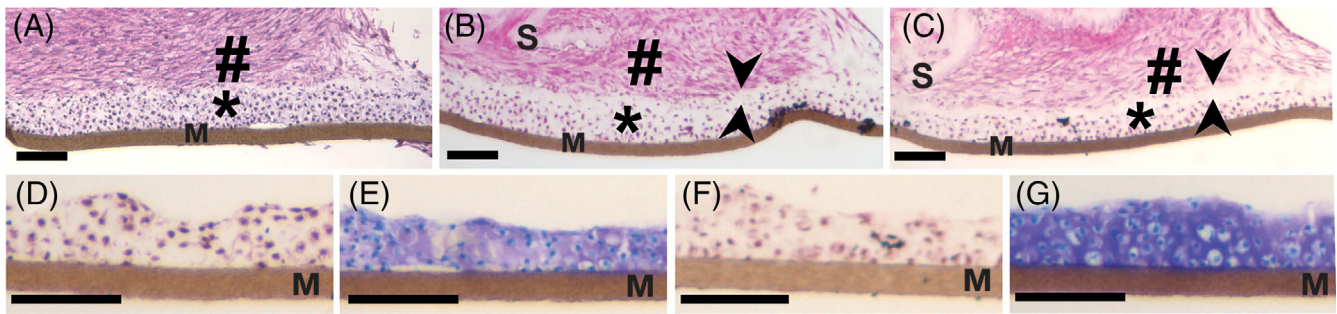


FIGURE 3 Histological images of interfaces that formed at 1 week between OAF tissues and either A, 3-day old, B, 5-day old, or C, 7-day old cartilage tissues. Histological appearance of 3-day, D,E, and 7-day, F,G, in vitro-formed cartilage prior to placement in coculture. S, PU scaffold; M, membrane support; #, OAF; *, cartilage; arrowheads indicate paucicellular layer tissue. H&E (A-C,D,F) and toluidine blue (E,G). Scale bars = 100 μ m [Correction added on 25 May 2020, after first online publication: Figure 3 has been corrected to reflect the label 'G' on the last image.]

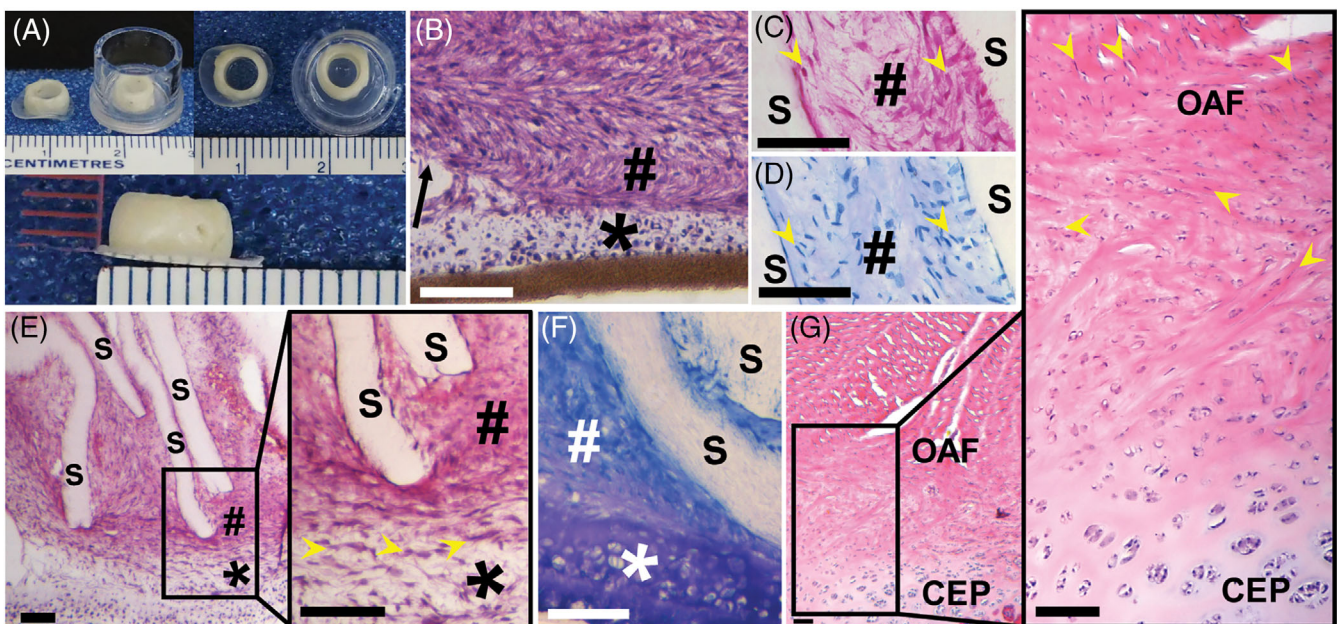


FIGURE 4 A, Lateral and top macroscopic views of 2-week cocultured OAF-CEP tissue constructs. Constructs are shown as they appeared both before and after removal from membrane insert holders. B, 2-week old OAF and 3-day old cartilage integrated by 1 week of coculture. Arrow indicates the outermost edge of the in vitro OAF. C, OAF tissue formed between two layers of PU-ADO scaffold in 2-week cocultured constructs, and D, did not stain for proteoglycan. E, Scaffold layers were oriented perpendicularly to the cartilage at the interface of 2-week OAF-CEP. The inset shows the indicated interface region at a higher magnification. F, Proteoglycans in the in vitro interface at 2 weeks of coculture were localized to the cartilage tissue layer (purple staining). G, Native bovine OAF-CEP interface. The inset shows the indicated interface region at a higher magnification. Yellow arrowheads indicate directional orientation of OAF cells in the in vitro model, C,D,E, and in the native interface, G. #, OAF; *, cartilage; S, scaffold. B,C,E-G: H&E. D and F: toluidine blue. Scale bars = 100 μ m

GAG, and OH-Pro, respectively. OH-Pro was converted to collagen assuming that the concentration of OH-Pro in collagen by weight is approximately 13%.³⁸ Collagen and GAG were normalized to DNA.

2.10 | Statistical analysis

Each experimental condition was performed in triplicate and was independently repeated at least three times using cells from different animals. Tensile testing was performed on 16 samples for 2-week OAF-CEP and 14 samples for 4-week OAF-CEP, from five independent experiments. Results are expressed as mean \pm SD. Data were not tested for normality.

Differences between groups were determined using an unequal variances t-test and considered to be statistically significant at $P < .05$.

3 | RESULTS

3.1 | Coculture of OAF on cartilage tissue generated an integrated tissue interface

2-week in vitro-formed OAF tissue placed in direct-contact coculture with 3, 5, or 7 day in vitro-generated cartilage formed integrated tissues by 1 week (Figures 3A-C). An acellular zone of ECM developed

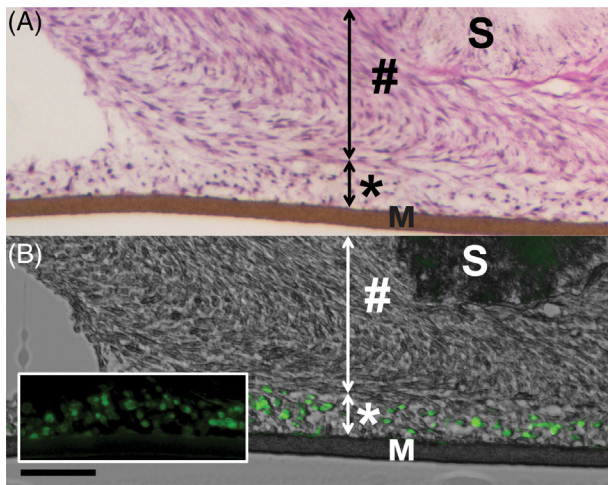


FIGURE 5 Histological images of the OAF-CEP interface at 2 weeks of coculture. Chondrocytes were prelabeled with CFDA. Light microscopical image, A, corresponds to the fluorescent microscopy image, B, which showed that the CFDA-labeled chondrocytes remained localized to the cartilage layer. #, OAF; *, cartilage; S, PU scaffold; M, membrane support. A, H&E; B, DIC/fluorescent microscopy. Scale bar = 100 μm . The OAF scaffold is weakly green autofluorescent

at the interface in the superficial aspect of the pregrown 5- and 7-day old cartilages (Figures 3B,C), appearing thicker in the latter. Neither 3- nor 7-day cartilages grown alone in Ham's F12 contained an acellular zone (Figures 3D-G), indicating that this zone was not a pre-existing characteristic of the older tissues. Based on this finding, all further experiments utilized 3-day old cartilage tissues to avoid the development of a cell-poor zone which could negatively affect integration between tissues.

Cocultured tissues integrated rapidly to form OAF-CEP constructs (Figure 4A). OAF tissues remained adherent to the cartilage tissues during media changes on day 2, suggesting that some degree of integration had occurred by this time. Histologically by 1 week, the tissues were integrated (Figure 4B). Histology also confirmed the presence of OAF-like tissue composed of elongated cells oriented parallel to PU-ADO scaffold fibers (Figures 4C,D). Scaffold layers were oriented perpendicularly to the cartilage tissue and OAF cells aligned parallel to the cartilage layer at the interface (Figure 4E), similar to the cell alignment seen in the native bovine interface (Figure 4G). Proteoglycan was not seen in the OAF tissue at 2 weeks as indicated by absence of toluidine blue staining (Figure 4D), but was present in the cartilage at the interface (Figure 4F). By 4 weeks, proteoglycans appeared to extend past the interface and into the OAF tissue as indicated by toluidine blue staining (data not shown).

3.2 | Chondrocytes remained localized to the cartilage tissue

Fluorescent labeled chondrocytes were localized to the cartilage layer and were not seen in the OAF of 2-week constructs (Figure 5).

Spindled cells resembling OAF cells were seen in the superficial aspect of the cartilage to intermingle with the fluorescent cells, suggesting that OAF cells grew down into the cartilage layer to form the interface.

3.3 | Immunohistochemical characterization of the bioengineered OAF-CEP interface

Immunostaining showed that in vitro-formed OAF tissue contained collagen type I and the cartilage contained collagen type II, similar to the localization seen in native bovine interface (Figure 6). Compared to 2-week old constructs, 4-week constructs showed more pronounced collagen type I staining in the OAF above the interface and coaccumulation of the two collagen types at the interface (indicated by yellow fluorescence; Figure 6E). Collagen type I and II colocalization was also seen in the native interface (Figure 6H).

Diffuse collagen type II staining was present in the in vitro OAF region just above the cartilage-like layer (white arrows; Figures 6B,E), which corresponded to the region where OAF cells were aligned parallel to the cartilage surface (white arrows; Figures 6A,D). Above this region, the OAF tissue only stained for collagen type I (green arrows; Figures 6B,E) and no collagen type II was detected in OAF tissue distal from the interface region.

Aggrecan was present in the cartilage layer. In some tissues, small amounts were seen in the interfacial OAF of the 2-week in vitro interface (Figure 6C). Aggrecan was present above the interface in the OAF tissue at 4 weeks of coculture (Figure 6F), resembling the native bovine OAF-CEP interface (Figure 6I).

3.4 | Apparent mechanical strength of the in vitro OAF-CEP interface increased over time

Pull-apart testing showed that the interfacial mechanical strength of 2-week cultured OAF-CEP was 11.9 ± 7.1 kPa, and significantly increased to 21.0 ± 8.3 kPa at 4 weeks ($P = .002$) (Figure 7). Histological examination of 2-week ($n = 3$) and 4-week ($n = 3$) samples that did not fully separate showed that failure occurred between the OAF and cartilage layer (Figures 7C,D). Mid-substance failure additionally occurred either within the cartilage ($n = 1$, Figure 7E) or within the OAF ($n = 1$, Figure 7F).

3.5 | No significant differences in DNA, collagen, or proteoglycan contents detected at the interface between 2 and 4 weeks of coculture

DNA content of the interface tissue was not significantly different between 2- and 4-week OAF-CEP constructs ($P = .27$). Similarly, DNA content of OAF or cartilage tissues cultured alone did not significantly change between 2 and 4 weeks (OAF: $P = .40$; cartilage: $P = .50$, Figure 8A).

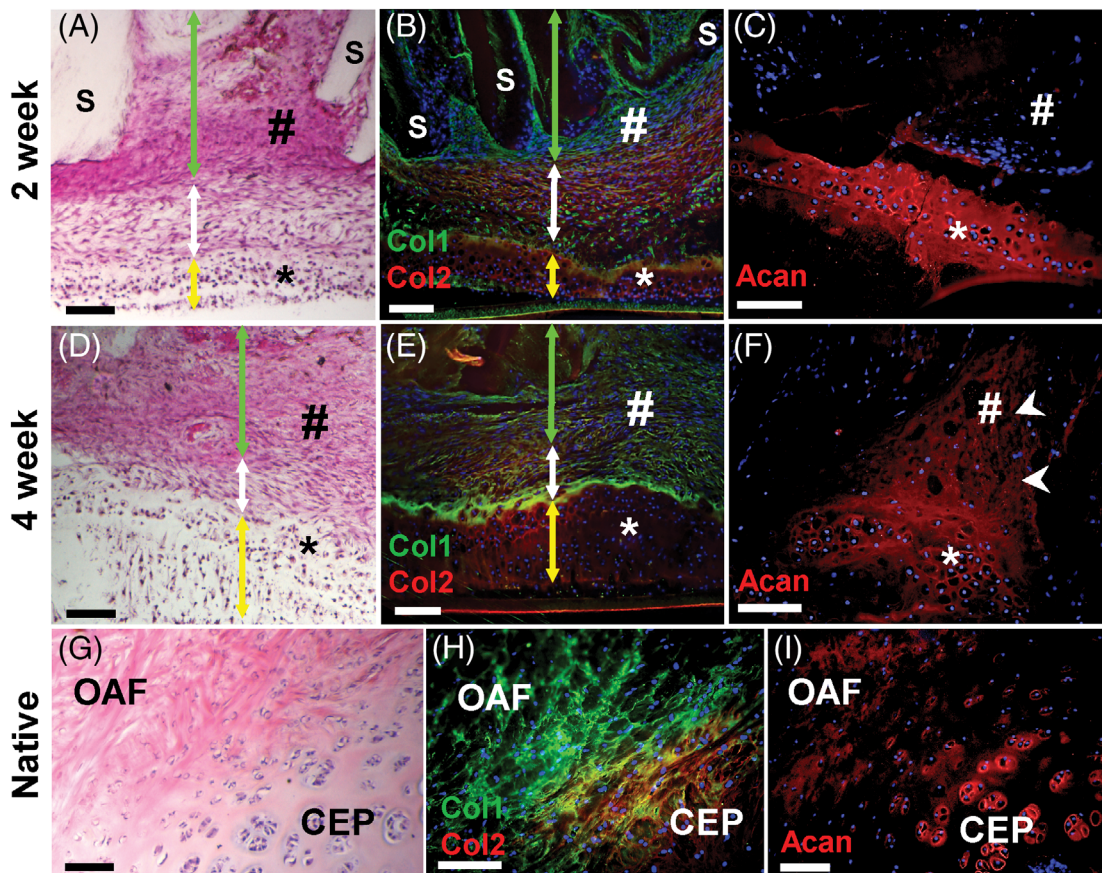


FIGURE 6 Representative histological images of the in vitro interfaces following staining by H&E, A,D,G, and immunostaining of corresponding sections for collagen type I (green) and type II (red), B, E, or aggrecan (red), C, F, of 2-week, A-C, and 4-week, D-F, cocultured constructs. Nuclei were stained with DAPI (blue). The native bovine OAF-CEP interface was visualized histologically following H&E staining, G, and by fluorescent microscopy after immunostaining for collagen type I (green) and type II (red), H, or aggrecan, I. Green arrows, in vitro OAF tissue; White arrows, interface region of in vitro OAF-like tissue; Yellow arrows, in vitro cartilage tissue; White arrowheads, presence of aggrecan in in vitro OAF region. #, in vitro OAF; *, in vitro cartilage; S, scaffold. Scale bars = 100 μ m

There were no significant differences in normalized GAG (as an indicator of proteoglycan; $P = .31$, Figure 8B) or collagen content ($P = .24$, Figure 8C) between 2 and 4 weeks of coculture.

4 | DISCUSSION

This study demonstrated that a model of an OAF-cartilage interface can be generated in vitro following direct-contact coculture of OAF tissue formed using multi-lamellar nanofibrous angle-ply PU-ADO scaffolds, with 3-day old cartilage tissue formed in 3D culture. Tissues appeared to attach by 2 days and could be handled at 1 week of coculture. Interface mechanical strength increased significantly over time. Chondrocytes did not migrate up into the OAF tissues, however OAF cells appeared to grow into the cartilage at the interface. OAF tissue of 2-week interface contained collagen type I, while the cartilage was rich in collagen type II and aggrecan. At 4 weeks, aggrecan was also present in the OAF above the interface. Collagen type II, normally not present in OAF tissues, was present in the OAF region at the interface at both 2 and 4 weeks. This collagen type II-positive

zone contained elongated cells within a loose ECM, suggesting that this tissue may have been derived from AF cells. This is the first study, to our knowledge, that describes the development of an engineered OAF-CEP tissue interface model which contains multiple key cellular and biomolecular attributes of the native interface.

The in vitro OAF-CEP model resembled the native interface in three ways. First, spindle-shaped OAF cells were aligned with the PU-ADO scaffold lamellae. This was also observed in a previous study in which fibronectin-coated PU-ADO nanofibers were shown to promote alignment of AF cells and collagen deposition parallel to the scaffold fibers using scanning electron microscopy and confocal microscopy.³⁹ OAF cells were aligned parallel to the cartilage at the interface, similar to the cell alignment described in the developing human fetal interface.⁴⁰ Chondrocytes remained localized to the cartilage and OAF cells appeared to grow downward into this tissue to form the interface, similar to the embryonic IVD development described for rats.⁴¹ Second, scaffold layers of the in vitro OAF-like tissue inserted vertically into the cartilage, modeling native AF-CEP insertion.¹¹⁻¹³ Vertical insertion at the native AF-CEP interface is important for tensile-to-shear stress transfer, as tensile stress (from

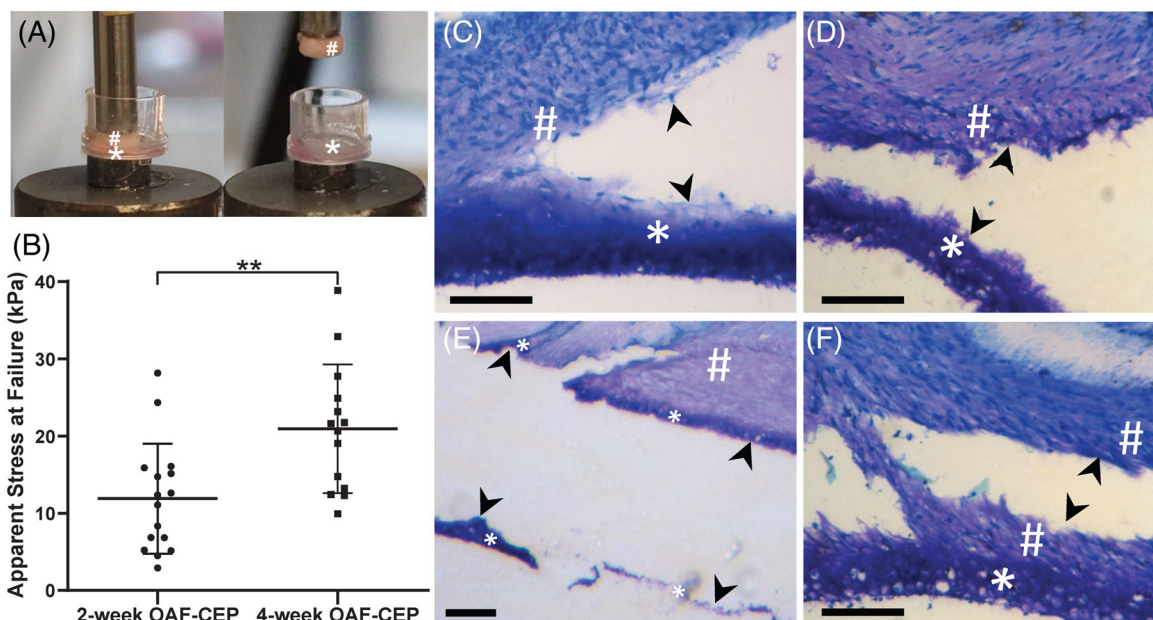


FIGURE 7 A, Macroscopic image of mechanical (pull-apart) testing of OAF-CEP constructs. B, Apparent stress at failure of 2- and 4-week cocultured constructs. Each point represents the apparent stress at failure of a single sample. $n = 16$ samples for 2-week OAF-CEP; $n = 14$ samples for 4-week OAF-CEP, from five independent experiments. Only tissues that completely detached were included in the calculations. Horizontal bars represent mean apparent stress values \pm SD for 2- or 4-week cocultured tissues. $**P = .002$. Histological images of failure site between the OAF and cartilage tissues of 2-week, C, and 4-week, D, cocultured constructs. Mid-substance failure occurred in either the cartilage, E, or the OAF, F, ($n = 1$ for each case). Arrowheads indicate regions of failure between tissues. #, OAF; *, cartilage. Toluidine blue. Scale bars = 100 μ m

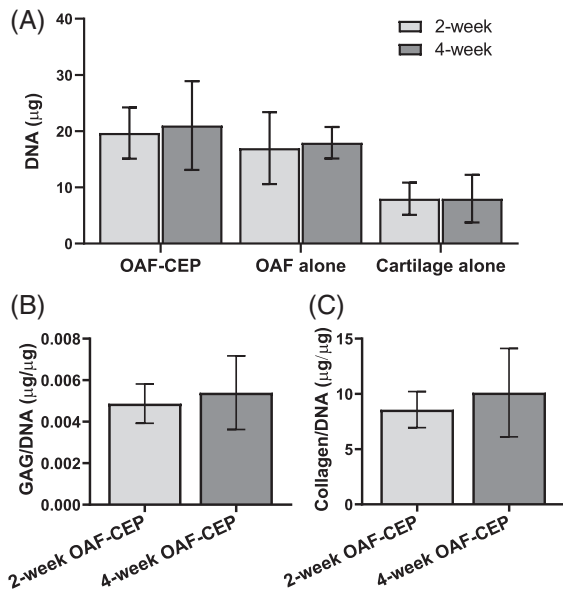


FIGURE 8 A, Biochemical quantification of DNA content of 2- and 4-week OAF-CEP interface tissues ($P = .27$), OAF or cartilage grown alone. B, GAG content/ μ g DNA of 2- and 4-week OAF-CEP interface tissues ($P = .31$). (C) Collagen content/ μ g DNA of 2- and 4-week OAF-CEP interface tissues ($P = .24$). $n = 10$ for 2-week OAF-CEP; $n = 11$ for 4-week OAF-CEP. Results expressed as mean \pm SD

cartilaginous ECM.^{11,14} Third, the general distribution pattern of collagen types I and II mimicked that of native bovine OAF-CEP, as shown previously¹⁵ and in the current study. Both collagen types were clearly visible at the interfacial region by 4 weeks, mimicking the native interface.

Collagen type I and type II colocalization has been linked to load transfer properties of the tendon-bone insertion site, another type of soft-tissue-bone interface. Collagen type I was found to be localized in the aligned fibers of the tendinous region (similar to the OAF) and to have higher tensile resistance than the fibrocartilaginous region adjacent to the bone insertion site, where collagen type II was colocalized with type I.⁴² Differences in biomechanical properties between the two regions were suggested to be directly related to their compositional organization, as unidirectional tensile stress is transferred along the tendinous aligned collagen type I fibers and subsequently distributed to the collagen type II/I-containing fibrocartilaginous matrix, which is less organized and therefore able to transfer multidirectional forces to the underlying bone.⁴² Although the tendon insertion is structurally different from the OAF-CEP interface, the overlap of collagen types I and II observed at the transition zone of the in vitro and in vivo OAF-CEP interface suggests that the composition of our model would enable it to appropriately distribute forces in a manner similar to what occurs physiologically.

Despite mimicking some structural and compositional features, this model did not fully reproduce native interface characteristics. Collagen type II was present in the OAF tissue adjacent to the interface, which is not characteristic of native OAF tissue. It is possible that the

spinal extension/flexion/lateral bending) is transferred into shear stress along the length of the AF fiber which is embedded within the

developing cartilage tissue may have induced these OAF cells to produce collagen type II by a crosstalk mechanism. Alternatively, collagen type II synthesized by the chondrocytes may have diffused into this looser AF-like tissue. Further study is required to determine which of these was occurring.

Structurally, the native AF-CEP interface demonstrates AF fiber anchorage through the CEP and into the VB.^{11,14} AF fibril interconnections with the CEP cartilaginous phase are strengthened by the CEP mineralized zone, which contributes to the interface's mechanical strength.^{11,14} In uniaxial tensile testing of native bovine VB-OAF-VB samples, failure never occurred at the OAF-CEP interface as observed in the current model. Instead it took place in the adjacent VB growth plate or OAF tissue, with failure stress values between 1.2 and 1.4 MPa depending on the number of lamellae present.⁴³ In comparison, the apparent mechanical strength of the current engineered model was 21 kPa, approximately 57 times weaker than native VB-OAF-VB segments containing six to ten lamellae.⁴³ Failure testing by Sapiee et al demonstrated that AF fibers pulled out VB osteons with them, indicating a high degree of AF-VB integration.¹⁴ Additionally, the transition from OAF to CEP in the native condition is much more gradual in comparison to the current model, which appears to occur in distinct layers (Figures 4E,G) and likely contributes to its lower comparative tensile strength. Future iterations of the model should aim to incorporate these native characteristics in order to enhance interfacial mechanical properties. Despite these differences, this model system will allow for studies on the first critical steps of integration that are necessary to develop mechanical stability following implantation of a bioengineered disc replacement.

Although there were no significant differences in ECM content of proteoglycan and collagen between 2 and 4 weeks of coculture, the apparent mechanical strength of the interface increased. There are several possible explanations for this. First, it may be that small changes in matrix accumulation along the interface were insufficient to be detected by the biochemical assays used. Second, despite using a standardized method of tissue dissection for all samples, it may be that variable amounts of tissue adjacent to the interfacial region were sampled for analysis, thereby masking small ECM changes that may have occurred specifically at the narrow interface region. Third, inherent variability within interface tissues, for example, in the form of discontinuities within integrated constructs or nonuniform macromolecular distribution along the length of the interface due to the presence of a scaffold layer, may also have limited the accuracy of biochemical quantification. Fourth, remodeling may have also contributed to the increase in apparent strength. Aggrecan monomers interact directly with collagen fibrils through their keratan sulfate-rich domains.⁴⁴ Increasing aggrecan-collagen interactions in the interfacial OAF over time may have enhanced the mechanical properties at this region. Matrix metalloproteinase (MMP) enzymes mediate ECM remodeling by regulating ECM protein degradation and cell migration.⁴⁵ Their specific roles in IVD interface development have not been extensively investigated. However, one study showed that MMP-1, MMP-2, MMP-3, and MMP-14 were more highly expressed in human fetal compared to postnatal IVDs (age 3-21 years), suggesting that

MMP-mediated ECM remodeling occurs during early tissue development.⁴⁶ Last, other factors not measured in this study may have contributed to the observed increase in tensile strength. Lysyl oxidase, an enzyme responsible for the formation of pyridinoline cross-links in collagen, has been suggested to improve integration strength between tissue-engineered and native cartilages.^{47,48} Thus, the observed increase in apparent mechanical strength may have reflected an increase in the number of collagen cross-links. Further study will be required to determine if this was occurring in these tissues.

One limitation of this study was that in order to obtain a sufficient number of cells for experiments, chondrocytes were obtained from cartilage harvested from articular joints rather than the thin IVD endplates. However, tissues from these two sources have some similarities.⁴⁹ Additionally, native CEP and in vitro cartilage generated from articular chondrocytes were each shown to have similar anabolic effects on in vitro-formed NP matrix proteoglycan accumulation,³³ suggesting that the use of articular chondrocytes was a suitable substitute for endplate chondrocytes in this model. Another possible limitation was that the OAF or CEP matrix contents distant to the site of integration were not quantified to determine if coculture conditions affected matrix accumulation by these tissues. Further study will be required to determine if there are any beneficial or detrimental effects of coculture on tissue beyond the interface.

In summary this is the first study, to our knowledge, that has established and characterized a tissue-engineered AF-CEP interface model that mimics the AF multi-lamellated angle-ply structure and reproduces some of the ECM features of the native interface. The ability to generate integration between in vitro OAF and cartilage tissues brings us one step closer toward the development of a fully integrated, multiphasic, biomimetic biological IVD implant suitable to use as a disc replacement. Additional studies will be required to address the integration of this implant with bone in vivo.

ACKNOWLEDGMENTS

This study was supported by CIHR (MOP142325). The authors would like to thank Meilin Yang for PU synthesis, Dr. Michael Floros for ADO synthesis, and Jian Wang for assisting with mechanical testing. The authors would also like to thank Harry Bojarski and Ryding-Regency Meat Packers for providing bovine tissues.

CONFLICT OF INTEREST

The authors state that there are no conflicts of interest for this study.

AUTHOR CONTRIBUTIONS

Jasmine E. Chong acquired and analyzed data, and wrote the manuscript. J. Paul Santerre and Rita A. Kandel obtained the grant funding to support this work and contributed to experimental design, interpretation of data, and critical revision of the manuscript. All authors have read and approved the final submitted manuscript.

ORCID

Rita A. Kandel  <https://orcid.org/0000-0003-4047-3913>

REFERENCES

- Luoma K, Riihimäki H, Luukkonen R, Raininko R, Viikari-Juntura E, Lamminen A. Low back pain in relation to lumbar disc degeneration. *Spine*. 2000;25(4):487-492.
- Adams MA, Roughley PJ. What is intervertebral disc degeneration, and what causes it? *Spine*. 2006;31(18):2151-2161.
- van den Eerenbeemt KD, Ostelo RW, van Royen BJ, Peul WC, van Tulder MW. Total disc replacement surgery for symptomatic degenerative lumbar disc disease: a systematic review of the literature. *Eur Spine J*. 2010;19(8):1262-1280.
- Parker SL, Mendenhall SK, Godil SS, et al. Incidence of low Back pain after lumbar discectomy for herniated disc and its effect on patient-reported outcomes. *Clin Orthop Relat Res*. 2015;473(6):1988-1999.
- Pennicooke B, Moriguchi Y, Hussain I, Bonassar L, Härtl R. Biological treatment approaches for degenerative disc disease: a review of clinical trials and future directions. *Cureus*. 2016;8(11):e892.
- Kandel R, Roberts S, Urban JP. Tissue engineering and the intervertebral disc: the challenges. *Eur Spine J*. 2008;17(Suppl 4):480-491.
- Cassidy JJ, Hiltner A, Baer E. Hierarchical structure of the intervertebral disc. *Connect Tissue Res*. 1989;23(1):75-88.
- Smith LJ, Nerurkar NL, Choi KS, Harfe BD, Elliott DM. Degeneration and regeneration of the intervertebral disc: lessons from development. *Dis Model Mech*. 2011;4(1):31-41.
- Bruehlmann SB, Rattner JB, Matyas JR, Duncan NA. Regional variations in the cellular matrix of the annulus fibrosus of the intervertebral disc. *J Anat*. 2002;201(2):159-171.
- Sivan SS, Wachtel E, Roughley P. Structure, function, aging and turnover of aggrecan in the intervertebral disc. *Biochim Biophys Acta*. 2014;1840(10):3181-3189.
- Rodrigues SA, Wade KR, Thambyah A, Broom ND. Micromechanics of annulus-end plate integration in the intervertebral disc. *Spine J*. 2012;12(2):143-150.
- Junhui L, Zhengfeng M, Zhi S, et al. Anchorage of annulus fibrosus within the vertebral endplate with reference to disc herniation. *Microsc Res Tech*. 2015;78(9):754-760.
- Rodrigues SA, Thambyah A, Broom ND. A multiscale structural investigation of the annulus-endplate anchorage system and its mechanisms of failure. *Spine J*. 2015;15(3):405-416.
- Sapiee NH, Thambyah A, Robertson PA, Broom ND. New evidence for structural integration across the cartilage-vertebral endplate junction and its relation to herniation. *Spine J*. 2018;19(3):532-544.
- Nosikova YS, Santerre JP, Grynepas M, Gibson G, Kandel RA. Characterization of the annulus fibrosus-vertebral body interface: identification of new structural features. *J Anat*. 2012;221(6):577-589.
- Park SH, Gil ES, Cho H, et al. Intervertebral disk tissue engineering using biphasic silk composite scaffolds. *Tissue Eng Part A*. 2012;18(5-6):447-458.
- Lazebnik M, Singh M, Glatt P, Friis LA, Berkland CJ, Detamore MS. Biomimetic method for combining the nucleus pulposus and annulus fibrosus for intervertebral disc tissue engineering. *J Tissue Eng Regen Med*. 2011;5(8):e179-e187.
- Bowles RD, Gebhard HH, Hartl R, Bonassar LJ. Tissue-engineered intervertebral discs produce new matrix, maintain disc height, and restore biomechanical function to the rodent spine. *Proc Natl Acad Sci U S A*. 2011;108(32):13106-13111.
- Nesti LJ, Li WJ, Shanti RM, et al. Intervertebral disc tissue engineering using a novel hyaluronic acid-nanofibrous scaffold (HANFS) amalgam. *Tissue Eng Part A*. 2008;14(9):1527-1537.
- Choy AT, Chan BP. A structurally and functionally biomimetic biphasic scaffold for intervertebral disc tissue engineering. *PLoS One*. 2015;10(6):e0131827.
- lu J, Massicotte E, Li S-Q, et al. In vitro generated intervertebral discs: toward engineering tissue integration. *Tissue Eng Part A*. 2017;23(17-18):1001-1010.
- lu J, Santerre JP, Kandel RA. Towards engineering distinct multi-lamellated outer and inner annulus fibrosus tissues. *J Orthop Res*. 2018;36(5):1346-1355.
- Nerurkar NL, Baker BM, Sen S, Wible EE, Elliott DM, Mauck RL. Nanofibrous biologic laminates replicate the form and function of the annulus fibrosus. *Nat Mater*. 2009;8(12):986-992.
- Nerurkar NL, Elliott DM, Mauck RL. Mechanics of oriented electrospun nanofibrous scaffolds for annulus fibrosus tissue engineering. *J Orthop Res*. 2007;25(8):1018-1028.
- Koepsell L, Remund T, Bao J, Neufeld D, Fong H, Deng Y. Tissue engineering of annulus fibrosus using electrospun fibrous scaffolds with aligned polycaprolactone fibers. *J Biomed Mater Res A*. 2011;99(4):564-575.
- Yang J, Yang X, Wang L, et al. Biomimetic nanofibers can construct effective tissue-engineered intervertebral discs for therapeutic implantation. *Nanoscale*. 2017;9(35):13095-13103.
- Martin JT, Kim DH, Milby AH, et al. In vivo performance of an acellular disc-like angle ply structure (DAPS) for total disc replacement in a small animal model. *J Orthop Res*. 2017;35(1):23-31.
- Martin JT, Gullbrand SE, Kim DH, et al. In vitro maturation and in vivo integration and function of an engineered cell-seeded disc-like angle ply structure (DAPS) for total disc arthroplasty. *Sci Rep*. 2017;7(1):15765.
- Bowles RD, Williams RM, Zipfel WR, Bonassar LJ. Self-assembly of aligned tissue-engineered annulus fibrosus and intervertebral disc composite via collagen gel contraction. *Tissue Eng Part A*. 2010;16(4):1339-1348.
- Moriguchi Y, Mojica-Santiago J, Grunert P, et al. Total disc replacement using tissue-engineered intervertebral discs in the canine cervical spine. *PLoS One*. 2017;12(10):e0185716.
- Hudson KD, Mozia RI, Bonassar LJ. Dose-dependent response of tissue-engineered intervertebral discs to dynamic unconstrained compressive loading. *Tissue Eng Part A*. 2015;21(3-4):564-572.
- Hamilton DJ, Seguin CA, Wang J, Pilliar RM, Kandel RA. Formation of a nucleus pulposus-cartilage endplate construct in vitro. *Biomaterials*. 2006;27(3):397-405.
- Arana CJ, Diamandis EP, Kandel RA. Cartilage tissue enhances proteoglycan retention by nucleus pulposus cells in vitro. *Arthritis Rheum*. 2010;62(11):3395-3403.
- Yang L, Kandel RA, Chang G, Santerre JP. Polar surface chemistry of nanofibrous polyurethane scaffold affects annulus fibrosus cell attachment and early matrix accumulation. *J Biomed Mater Res A*. 2009;91(4):1089-1099.
- Theodoropoulos JS, De Croos JN, Park SS, Pilliar R, Kandel RA. Integration of tissue-engineered cartilage with host cartilage: an in vitro model. *Clin Orthop Relat Res*. 2011;469(10):2785-2795.
- Kawamoto T. Use of a new adhesive film for the preparation of multipurpose fresh-frozen sections from hard tissues, whole-animals, insects and plants. *Arch Histol Cytol*. 2003;66(2):123-143.
- Dyment NA, Jiang X, Chen L, et al. High-throughput multi-image cryohistology of mineralized tissues. *J Vis Exp*. 2016;Sept 14(115):e54468. <https://doi.org/10.3791/54468>.
- Ignat'eva NY, Danilov NA, Averkiev SV, Obrezkova MV, Lunin VV, Sobol' EN. Determination of hydroxyproline in tissues and the evaluation of the collagen content of the tissues. *J Anal Chem*. 2007;62(1):51-57.
- Attia M, Santerre JP, Kandel RA. The response of annulus fibrosus cell to fibronectin-coated nanofibrous polyurethane-anionic dihydroxyoligomer scaffolds. *Biomaterials*. 2011;32(2):450-460.
- Peacock A. Observations on the prenatal development of the intervertebral disc in man. *J Anat*. 1951;85(3):260-274.
- Hashizume H. Three-dimensional architecture and development of lumbar intervertebral discs. *Acta Med Okayama*. 1980;34(5):301-314.
- Thomopoulos S, Williams GR, Gimbel JA, Favata M, Soslowsky LJ. Variation of biomechanical, structural, and compositional properties

- along the tendon to bone insertion site. *J Orthop Res.* 2003;21(3): 413-419.
43. Rok ER. 2015. *Developing an in vitro model of the OAF-CEP interface: Towards tissue engineering the intervertebral disc* (MAsc thesis). Institute of Biomaterials and Biomedical Engineering, University of Toronto, Toronto, ON.
44. Hedlund H, Hedbom E, Heinegrd D, Mengarelli-Widholm S, Reinholt FP, Svensson O. Association of the aggrecan keratan sulfate-rich region with collagen in bovine articular cartilage. *J Biol Chem.* 1999;274(9):5777-5781.
45. Page-McCaw A, Ewald AJ, Werb Z. Matrix metalloproteinases and the regulation of tissue remodelling. *Nat Rev Mol Cell Biol.* 2007;8(3): 221-233.
46. Rutges JP, Nikkels PG, Oner FC, et al. The presence of extracellular matrix degrading metalloproteinases during fetal development of the intervertebral disc. *Eur Spine J.* 2010;19(8):1340-1346.
47. Eyre DR, Paz MA, Gallop PM. Cross-linking in collagen and elastin. *Annu Rev Biochem.* 1984;53:717-748.
48. Athens AA, Makris EA, Hu JC. Induced collagen cross-links enhance cartilage integration. *PLoS One.* 2013;8(4):e60719.
49. Moore RJ. The vertebral endplate: disc degeneration, disc regeneration. *Eur Spine J.* 2006;15(Suppl 3):S333-S337.

SUPPORTING INFORMATION

Additional supporting information may be found online in the Supporting Information section at the end of this article.

How to cite this article: Chong JE, Santerre JP, Kandel RA.

Generation of an in vitro model of the outer annulus fibrosus-cartilage interface. *JOR Spine.* 2020;3:e1089. <https://doi.org/10.1002/jsp2.1089>